


Article

Performance Analysis of Enhanced 3D Printed Polymer Molds for Metal Injection Molding Process

Khurram Altaf ^{1,*} , Junaid A. Qayyum ², A. Majdi A. Rani ², Faiz Ahmad ², Puteri S. M. Megat-Yusoff ², Masri Baharom ¹, A. Rashid A. Aziz ¹, Mirza Jahanzaib ³ and Randall M. German ⁴

¹ Center for Automotive Research and Electric Mobility (CAREM), Department of Mechanical Engineering, Universiti Teknologi PETRONAS, Bandar Seri Iskandar 32610, Perak, Malaysia; masrib@utp.edu.my (M.B.); rashid@utp.edu.my (A.R.A.A.)

² Department of Mechanical Engineering, Universiti Teknologi PETRONAS, Bandar Seri Iskandar 32610, Perak, Malaysia; junaid.ahmad_g03515@utp.edu.my (J.A.Q.); majdi@utp.edu.my (A.M.A.R.); faizahmad@utp.edu.my (F.A.); puteris@utp.edu.my (P.S.M.M.-Y.)

³ Department of Industrial Engineering, University of Engineering & Technology Taxila, Taxila 47080, Pakistan; jahan.zaib@uettaxila.edu.pk

⁴ Department of Mechanical Engineering, San Diego State University, San Diego, CA 92182, USA; randgerman@gmail.com

* Correspondence: khurram.altaf@utp.edu.my; Tel.: +60-14-940-2647

Received: 11 April 2018; Accepted: 29 May 2018; Published: 8 June 2018



Abstract: Conventionally, molds for metal injection molding (MIM) process are fabricated using metallic materials using conventional machining processes. Machined metal molds are resilient and therefore could be suitable for mass production of MIM parts. However, with the process of mass production leading to permanent hard tooling, the design is subjected to rigorous testing and iteration before finalization. During design analysis and the iteration process, the demand for MIM parts (part demand) is at low-volume. Therefore, machined metal molds could be costly and time consuming for low volume and customized end-use products. 3D printed molds could be a suitable choice for MIM production for such applications. The present study compares the performance of Fused Deposition Modelling (FDM) 3D printing (3DP) process made polymer molds with an aluminum mold for potential use in MIM process. It was observed that 3DP molds could successfully be used for a limited number of MIM cycles.

Keywords: 3D printing; rapid tooling; fused deposition modeling; sintering; metal injection molding; electro-less plating

1. Introduction

Mold making is one of the major bottleneck processes in the overall metal injection molding (MIM) process. Normally, molds for the MIM process are metallic and are made through machining. The machining process is time consuming and cost- and skill-intensive due to its inherent demands for labor effort, time, and material. However, machined metal molds are robust and suitable for high-volume part demand. However, for applications where part demand is customized, or design change is frequent and part requirements are low, the mold could become useless as soon as the demand is met. Even for mass production and high-volume demands of MIM parts, the design is subjected to rigorous testing, analyses, and prototyping before finalizing and permanent hard tooling, because once the mold is machined, it is quite difficult to implement any modification in the design. Therefore, prior to permanent hard tooling, soft tooling could be a good option for design validation and analysis.

Rapid tooling (RT) is defined as use of AM process for making molds, inserts, patterns, or auxiliary mold components. This could be direct, like the fabrication of molds or inserts for injection molding, or indirect, like the making of sacrificial patterns for casting [1]. RT can produce customized molds quickly with less effort. Most promising and reliable applications of 3D printed molds are related to highly tailored but low-volume part demand. 3D printed polymer molds could be used for indirect rapid tooling for such demand [2]. Nevertheless, if the part demand is low, 3D printed polymer molds could be viable for direct rapid tools, whereas the machine mold could become redundant due to low demand. 3D printed polymer molds could find their scope with high volume, customized MIM parts, mainly in two ways: first, as direct rapid tools, to be made rapidly and disposed of after completing permissible number of MIM cycles; and secondly, as precursors for permanent hard tooling. Metal molds are most promising in the high volume demand of standardized parts. 3D printed polymer molds could be used for product development, performance testing of MIM parts, and design analysis of molds. Once the design is finalized, mold could be machined for a series production of standard parts. Thus, the product development and process development cycles are synergistically deployed to optimize overall manufacturing cycle. Performance of polymer molds as investment casting patterns and patterns for silicone molding has been reported in some studies [3].

Dixit et al. presented the statistical models developed regarding the behavior of tooling and end-use parts made through conventional and modern machining. Also discussed in the paper is a comprehensive review of various approaches of material behavior modelling. They explained that the material behavior modelling has a great influence on the process design, tools, and the final product. The material and manufacturing models are critically investigated to ensure optimum performance of the end-use parts; however, for low-volume or prototype production, empirical models could also be acceptable [4]. Nevertheless, unlike forming or machining processes, the material models for the FDM process, though reported in some studies, are largely empirical in nature [5]. The heat dissipation and cooling of the MIM green-part could be a potential challenge in these molds. However, for a limited number of MIM cycles, these downsides could be overlooked. Still, optimum selection of process parameters of mold manufacturing and selection of superior RT process has been known to reduce the challenge [6]. Effects of introduction of popular metals like iron [7,8] and copper [9] have been investigated for FDM manufacturing through non-proprietary composite filaments. It was learnt that these enhanced filaments could be efficiently used in existing FDM platforms and are promising for the manufacture of MIM molds. FDM manufacturing through ceramic-polymer composited feedstock is a baseline study with which to make prospective MIM molds [10,11].

There are many studies that have investigated polymer injection molding by employing FDM molds. These studies have investigated comprehensively the improvement in strength or the heat transfer rate of the FDM filament through material or design enhancement. However, any direct effects on thus-made end-use parts were not investigated [12]. A few studies analyzed the properties of MIM parts made through FDM made polymer molds. Khurram et al. [13] investigated the potential of FDM-produced ABS mold for the MIM of copper-based feedstock. These studies were, however, focused on MIM of copper-based feedstock only, and these studies did not carry results regarding testing of MIM parts. In the present study, potential of FDM-produced ABS and nylon molds has been carried out. The effects of mold material on feedstock filling and mechanical properties have been reported.

The approach of using FDM-produced polymer molds for functional prototyping and/or for low-volume demands of functional parts is promising for addressing challenges of mold machining for customized and low-volume MIM demands. However, this approach has two major challenges. First, it is suitable for low-volume demands of end-use parts, and secondly, these molds are specifically dedicated for the MIM process. For manufacturing processes like casting and similar processes, these molds cannot be used directly as they have been used in the present study. Rather, these molds could be used to make sacrificial patterns, which could be used in investment casting [1]. Molds could be made according to any complex and intricate design to perform MIM. However, in the present study,

the mold cavity is printed according to ASTM standard for tensile testing of MIM parts so that the comparison with the benchmark MIM parts could be done. Some studies have reported that tailored machines and methods could also produce results, truly comparable to the standardized methods. Their results indicated that the suggested compression testing machine equipped with a logistic cam profile can successfully replicate the operating conditions of the other testing machines [14]. Krahmer et al. presented their work on determining the effects on surface state and tensile test performance occurred as a result of manufacturing method, working with low-carbon steel as the study material. Moreover, they concluded that it is not always mandatory to analyze the performance with acceptable mechanical testing could also be displayed by the specimens manufactured through non-conventional methods while being sustainable [15]. Likewise, non-conventional manufacturing processes could be equally suitable for mold making, and AM/3DP being one of them as discussed in the present study.

From the previous studies about the application of rapid tools for injection molding, it was learnt that either metallic molds were used in combination of polymer injection molding, or polymer molds were used for polymer injection molding [7,16,17]. In a study by King et al. [18], bronze-filled modular tool inserts were compared against the conventional mold inserts. Masood et al. [7] used iron-infused nylon filament to make molds through the FDM process. Molds made through this composite filament were used for injection molding of LDPE feedstock. Some other studies reported use of polymer molds for polymer sheet processing [19]. A similar study was done using Poly Lactic Acid (PLA) and Acrylonitrile butadiene styrene (ABS) molds with copper-based feedstock. However, the conclusions drawn regarding performance of polymer molds were qualitative in nature, and testing of molded parts was not performed [20].

In the current study, the new concept of polymer mold and metal feedstock was used to investigate the performance of the polymer molds. The polymer molds made of ABS and nylon were used for metal injection molding using stainless steel 316L-based feedstock. The design and surface of the molds were enhanced to analyze enhancement effects on the MIM performance of molds. Furthermore, the conclusions regarding the performance of molds were drawn based on comparing the mechanical properties of MIM parts molded through polymer molds, with the benchmark parts molded through aluminum mold, as well as with the literature values. As per the analysis of the above studies, it could be concluded that the current study is new and unique.

2. Materials and Methods

The mold insert was housed in the mold block to produce the mold assembly. Complete mold assembly was produced through FDM process using polymer materials. The mold block was made of ABS filament, whereas two mold inserts were made of ABS and nylon each. This configuration facilitates the changing of mold insert while keeping the same mold block. In case the mold insert has undergone some distortion after a number of MIM cycles, it could be replaced in the mold block. A cover plate was fabricated and placed on the top of mold block with an aluminum plate fixed in the cover plate to assist feedstock flow and heat dissipation from the feedstock. Enhancements in surface and design of mold inserts were made to reduce adhesion of feedstock with the mold wall and to facilitate the part release. Surface was enhanced through copper plating, whereas design was enhanced by making mold insert as split into two halves. Materials for surface enhancement included acrylic acid, hydrochloric acid, copper sulfate, Phenyl-amine-dihydrogen-chloride, ammonium hydroxide, sodium hydroxide, sodium nitrite, sodium borohydride, and sodium tartrate. Figure 1a,b show the Computer Aided Design (CAD) model and FDM mold block with insert.

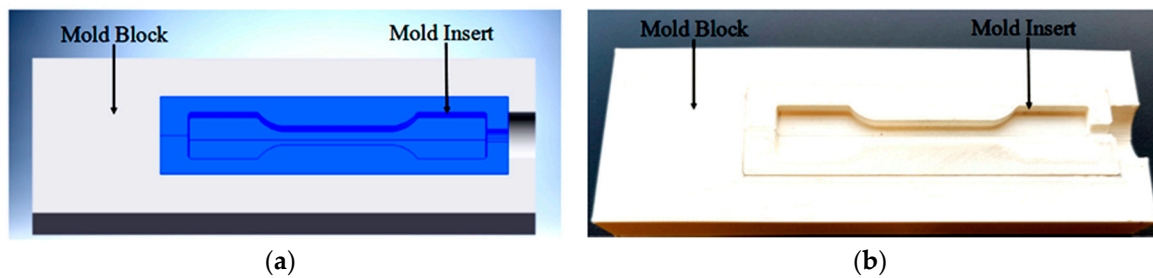


Figure 1. (a) CAD model of mold assembly and (b) FDM printed mold assembly.

2.1. Surface Enhancement

ABS mold insert was plated with copper through polymer grafting process, which is a process for coating of difficult substrates, typically polymers. Recently, copper grafting on ABS substrates has been studied in detail [21]. The metal deposition occurs in three steps. The first step involves the grafting of surface with acrylic acid in the presence of 0.1 M solution of 1.4 phenyl amine dihydrogen chloride in 0.5 M HCl and 0.1 M aqueous solution of sodium nitrite. Both the solutions were mixed in equal proportion in the equal volume of acrylic acid. ABS mold inserts were placed in the solution at 40 °C for 3 h. This process grafts a layer of acrylic acid on the ABS surface. After sonication in sodium hydroxide and deionized water for 10 min, the mold insert was subjected to another solution for reduction of copper ions on carboxylic functional group of acrylic acid. The reducing solution was comprised of 0.1 M copper sulfate, 0.1 M sodium borohydride, 0.1 M sodium hydroxide, and 0.6 M ammonium hydroxide. ABS mold inserts were placed in the reducing solution at 40 °C for 20 min to allow formation of copper seed layer on the polar acid functional group. Finally, the seed-layer was further reinforced when the inserts were placed in the electro-less metal deposition solution. Volume of the electro-less deposition (ELD) solution was 250 mL and contained 2.5 g, 3 g, 2.5 mL, and 4.5 g of copper sulfate, sodium hydroxide, formaldehyde, and sodium tartrate, respectively. Figure 2 shows the copper plated ABS mold insert. ABS was coated with copper, because it is prone to adhesion with the feedstock, as it has heat deflection temperature of 98 °C. However, nylon has heat deflection temperature of 160 °C and thus is relatively safe from adhesion with feedstock. Therefore, no metal plating was carried out for nylon mold inserts. Figure 3 indicates the electro-less plating process flow for ABS material.

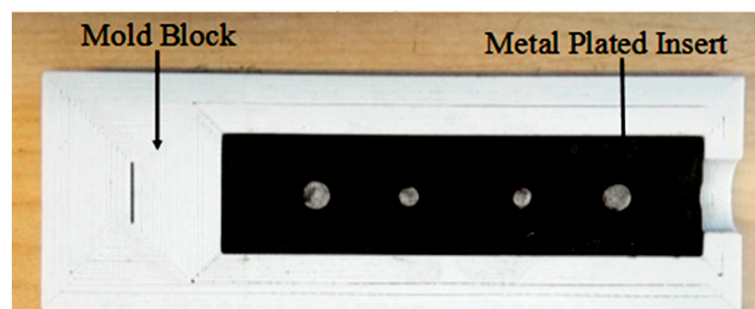


Figure 2. Metal plated ABS mold insert.

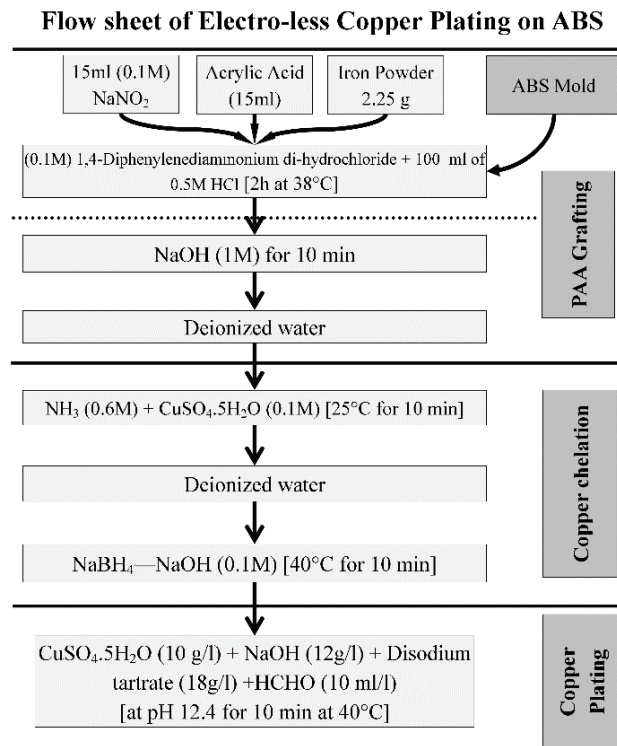


Figure 3. Copper plating on ABS through grafting process.

2.2. Design Enhancement

For design enhancement and modification, the mold insert was split into two equal sections vertically. Each half was made through FDM process and was assembled together in the mold block. Polymer mold inserts could slightly swell during molding filling process, and the heated feedstock could adhere to the surface of mold insert. Therefore, adhesion force in releasing MIM part from the mold insert could result in part failure. The split configuration in mold inserts is attributed to part release with much less ejection force. The mold insert is split in two halves so that it could be separated to part release once MIM cycle is complete. Figure 4a,b show the design enhancement in the ABS and nylon mold inserts.

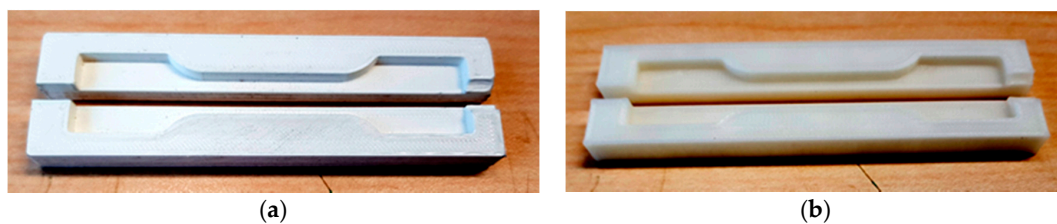


Figure 4. (a) ABS split mold insert and (b) nylon split mold insert.

2.3. Preparation of MIM Feedstock

Stainless steel 316L metal powder was the key component for the feedstock. Polypropylene was used as binder and stearic acid as surfactant, and paraffin wax was used to facilitate feed stock flow during molding. In mixing step, 9.3 g of stearic acid was mixed with 3.8 kg of 316L steel powder in turbular mixer for 90 min. Then, 133 g of paraffin wax was heated in Z-blade mixer for 30 min at 70 °C and at 40 rpm. The 316L powder, already mixed with stearic acid, was then allowed to mix with the paraffin wax in Z-blade mixer for 30 min. Finally, polypropylene binder was mixed in the above mixer at 170 °C at 60 rpm for 90 min.

2.4. Metal Injection Molding

MIM was carried out using the vertical injection molding machine (MCP Tooling model MCP-100KSA, SLM Solutions, Lübeck, Germany), at standard conditions of temperature and pressure of 170 °C and 4.5 bar, respectively [22]. The filling of benchmark molds was good and almost complete due to the good surface quality. However, the RT polymer molds offered resistance to the flow of feedstock due to relatively rough surface, which is inherent challenge in the FDM manufactured parts. However, slight increase of injection temperature leads to comparable mold filling. Copper plating was effective at controlling the adhesion of feedstock with the mold; however, it increased the resistance to the feedstock flow, due to which molding in copper-plated ABS mold was performed at elevated temperature. The mold was held in the clamps at the bottom of the heating chamber, and the feedstock was injected from the top chamber. Machine was operated in manual mode, since prototyping MIM is more effective in manual mode. Injection time was kept at 10–15 s so that complete filling of mold cavity could be ensured. After MIM, once the pressure gauge got stable, mold was released from the clamps. On cooling, mold sections were separated, and mold insert was ejected to release green part. The same process was repeated for subsequent MIM cycles. The MIM part was, according to ASTM E8M-00, standard. Table 1 below presents the MIM process parameters.

Table 1. Process parameters for MIM.

Injection Molding Parameters	Units	Benchmark Metal Mold	Copper-Plated ABS Mold	Split-ABS Mold	Split-Nylon Mold
Injection pressure	bar	4.5	4.5	4.5	4.5
Injection temperature	°C	170	200	180	175
Injection time	second	11–15	11–15	11–15	11–15
Mold initial temperature	°C	25	45	45	45

2.5. De-Binding and Sintering

The de-binding process refers to removal of binder from the feedstock. Typically, de-binding takes places in two steps: viz. solvent and thermal de-binding. During solvent de-binding, specimens were placed in n-heptane liquid at 50 °C for 4 h in water bath (Protech, model 830-S1, Tech-lab Sdn. Bhd., Balakong, Malaysia). This dissolves the polypropylene binder to some extent in the n-heptane liquid. Rest is sublimed during thermal de-binding. The de-binding and sintering processes are depicted in Figure 5a,b.



Figure 5. (a) Solvent de-binding of MIM green parts and (b) furnace for thermal de-binding and sintering of MIM brown parts.

Thermal de-binding and sintering were integrated in the combined cycle and conducted using high temperature furnace (MTI Corporation, model GSL-1700X-s, Richmond, CA, USA).

Thermal de-binding takes place during gradual heating up to 500 °C in 350 min, and the temperature was retained for 150 min. The temperature was increased to 900 °C in 120 min and was held for 105 min. Then temperature was further raised to 1130 °C in 103 min and was held for another 105 min. Then, temperature was increased to 1250 °C in 180 min and was held for 200 min to ensure proper sintering. Finally, the furnace was allowed to cool at 5 °C/min to avoid heat driven buckling, caused by rapid cooling. The sintering cycle is shown in Figure 6.

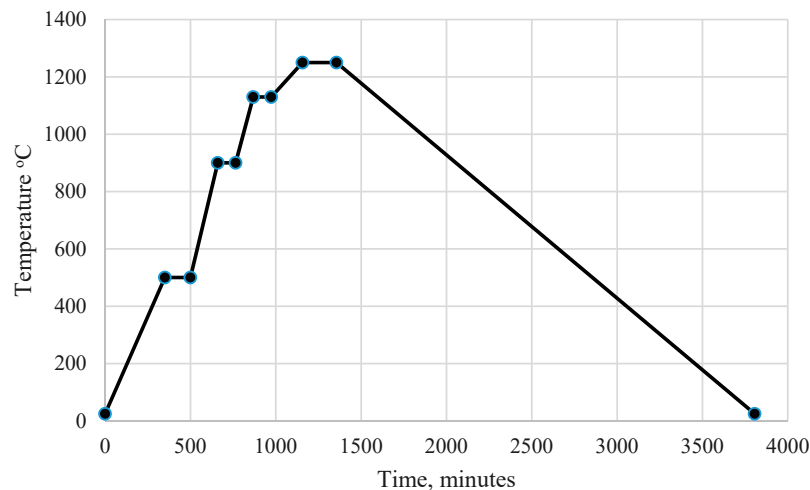


Figure 6. Combined cycle for thermal de-binding and sintering of MIM brown parts.

2.6. Tensile Testing

Tensile testing was carried out for MIM parts produced by metal and polymer mold inserts. This was done to compare the sintered part properties produced with metal and polymer molds. Tensile testing was carried out according to ASTM E8M-00 standard with strain rate kept as 2 mm/min. The strain rate was kept low to avoid generation of heat in the specimen, which could introduce error in the measurement. The tensile testing machine (Amsler Zwick/Roell 100KN, Ulm, Germany) was equipped with load cell and extensometer to measure local and global extension. Stress-strain curve was plotted by the machine built-in software. All tensile tests were carried out at room temperature and humidity level of 50% [23]. Tensile testing is indicated in Figure 7a,b.

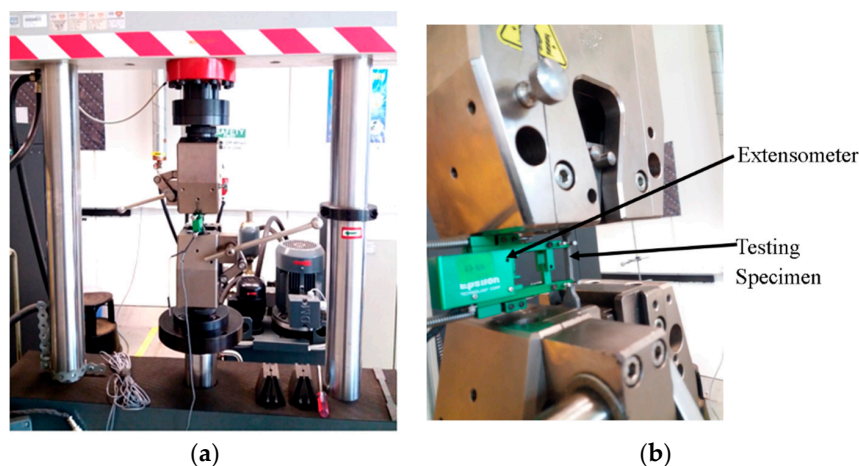


Figure 7. (a) Tensile test machine and (b) sample fitted in the machine.

2.7. Surface Hardness Testing

For the hardness testing, ASTM E92-17 standard was used to measure surface hardness of the sintered specimens. MIM parts molded in metal, ABS, and nylon molds were subjected to measurement of surface hardness. Hardness tests were conducted on Vickers Hardness testing machine (Micro-hardness tester, Leco Corp. model LM-700AT, St. Joseph, MI, USA). For all the samples molded through metal, ABS, and nylon molds, Vickers hardness tests were performed with test load of 500 gf and dwell time of 15 s. F being applied force and d being average of indenter diagonals. Hardness tests were performed at three different locations, and the reported values were calculated by taking the average of the recorded values. The Vickers hardness was computed as shown in the formula below.

$$HV = \frac{1.854 F}{d^2} \quad (1)$$

2.8. Density Measurement

The density of sintered part is attributed to the packing of powder during sintering, as well as filling of feedstock during molding. Density measurement was performed on sintered parts produced with aluminum, ABS, and nylon mold inserts. The density measuring instrument has two pans, one in water and the other in the air. Equal volume of same sample is placed in both the pans, and the machine measures the relative density by buoyancy offered to the sample. ASTM B962-17 standard was used for the density measurement of sintered parts. A density measuring instrument was used to measure the density of specimens. The samples were cleaned with methanol and dried in ambient air. The samples were then weighed before and after soaking. Finally, samples were weighed while immersed in the jar. If ' w ' denotes weight of sample in air, ' m ' denotes weight of sample in auxiliary liquid, ρ_L is density of auxiliary liquid, and ρ_o is the air density; the density ρ_s can be calculated from the following expression below.

$$\rho_s = \frac{w}{w - m}(\rho_L) \quad (2)$$

3. Results

3.1. Metal Injection Molding

MIM was carried out with aluminum mold as a benchmark to compare performance of polymer molds with it. Green-part failure rate in the metal mold was less than polymer molds. Generally, surface quality of MIM parts is good, except for the presence of impressions of mold ejector pins. Figure 8 shows the aluminum mold with green and sintered parts.

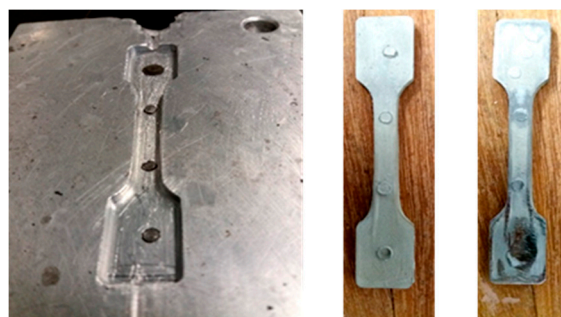


Figure 8. Aluminum mold with green and sintered MIM parts.

Metal injection molding using SS 316L feedstock was successfully carried out for all mold inserts. The surface finish of copper-plated ABS mold insert was not as smooth as aluminum mold, yet complete filling into the mold cavity was achieved after experimenting with the injection

parameters. However, challenges in the release of the green-part were still present in copper-plated ABS mold insert. De-binding and sintering of the green-part was successfully carried out, and the sintered part got the characteristic shiny appearance. Figure 9 shows the copper plated mold with green and sintered parts.

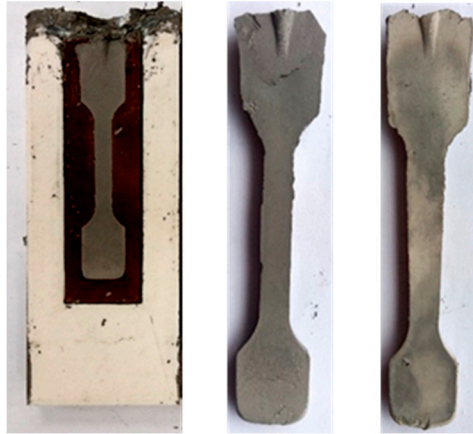


Figure 9. Copper plated ABS mold with green and sintered MIM parts.

Split ABS mold insert had better surface finish compared to the copper plated ABS insert; hence filling of feedstock was successful. Complete filling of feedstock was observed in the split ABS insert. The inherent advantage of split ABS insert is that it can be opened from the split line to release the green part once the injection is complete. This releases green-part with less force, thereby preserving the part integrity and reducing the part failure chances. Figure 10 shows the split ABS mold with green and sintered parts.



Figure 10. ABS split mold with green and sintered MIM parts.

The performance of nylon insert was better compared with the copper plated ABS mold insert due to the high heat deflection temperature and strength. The release of green part was better in nylon insert, and the part was strong enough to successfully undergo de-binding and sintering without failure. Characteristic metallic surface was visible in the sintered part. Nevertheless, mold packing line was visible in the green-parts, which demand some post-processing for better quality. Figure 11 shows the split nylon mold with green and sintered parts.



Figure 11. Nylon split mold with green and sintered MIM parts.

3.2. Tensile Tests

3.2.1. Aluminum Molded Parts

Parts molded using aluminum mold displayed good performance, as the elastic limit, yield point, and ultimate strength are all clearly identified from the stress-strain curve. These parts are more ductile and elastic in nature. Two main reasons for this behavior are rigidity of the mold and good heat dissipation. Aluminum mold rigidity allows accommodation of sufficient feedstock in the cavity without any swelling. This, in turn, makes dense compaction possible in the aluminum mold. Cooling of green part is quick in aluminum mold, due to which powder particles settle quickly and may have better density.

3.2.2. Copper Plated ABS Molded Parts

The MIM parts molded through copper-plated ABS mold insert showed dissimilar behavior compared to other molded parts. The slope of stress-strain curve is comparatively less, which implies that stiffness is less. The fracture stress is 284 MPa, which is still closer to the polymer molded MIM parts. However, fracture deformation is less, which clearly implies brittleness, although it should be noticed that the modification in the sintering cycle could be tailored to gain desired properties. One noticeable matter that is the changed behavior of stress-strain curve for this part could be the reason of lower densification as compared to other polymer inserts molded parts.

3.2.3. Split-ABS Molded Parts

Parts molded using split-ABS insert displayed similar behavior to the bench mark part within the elastic region. The split mold insert has the capability to expand slightly to accommodate enough feedstock and to allow sufficient packing of particles. The elastic limit, yield strength, and ultimate strength are all clearly identifiable in the graph. Elasticity is more than parts molded in split-nylon insert, but less than bench mark parts. The ultimate strength is marginally less, yet still comparable to the rest of the parts.

3.2.4. Split-Nylon Molded Parts

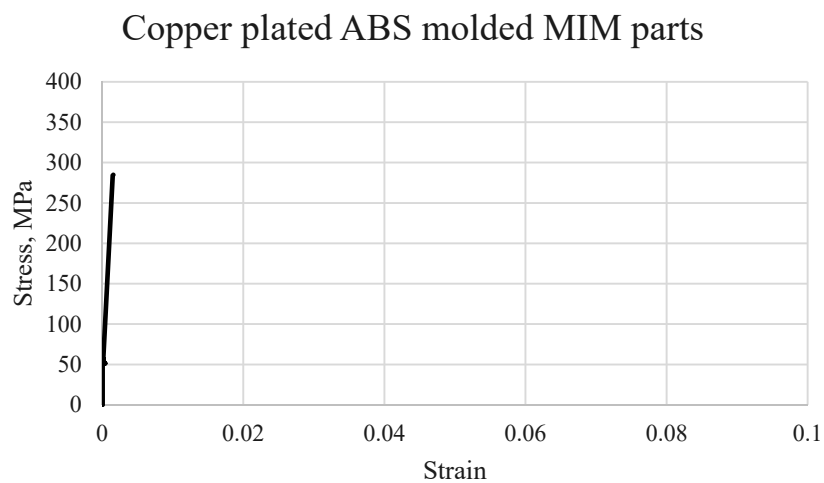
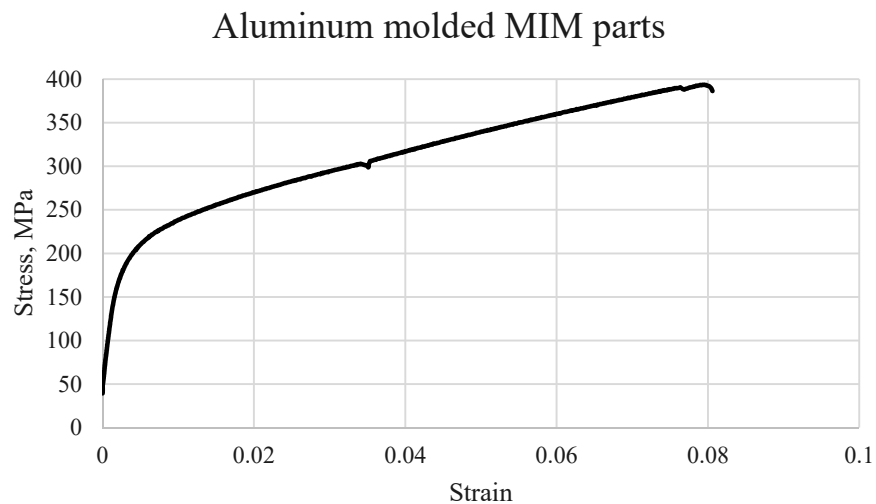
Regarding elastic limit, yield strength, and ultimate strength, similar characteristics were observed for the specimens made through split-nylon molds. Though these parts displayed less elasticity than the rest, but the ultimate strength was better than ABS molded specimens. Another noticeable characteristic of the nylon insert MIM part is that the fracture strain is less than the other MIM parts.

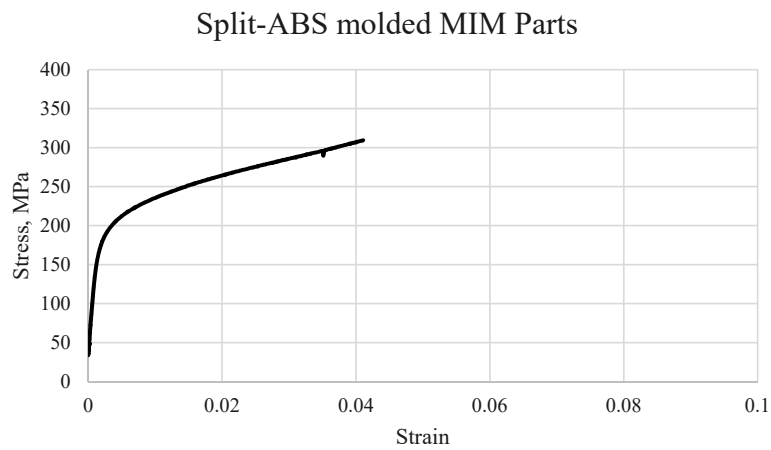
The Table 2 below is indicated some of the major mechanical properties of the sintered parts.

Table 2. Comparison of major mechanical properties for MIM parts.

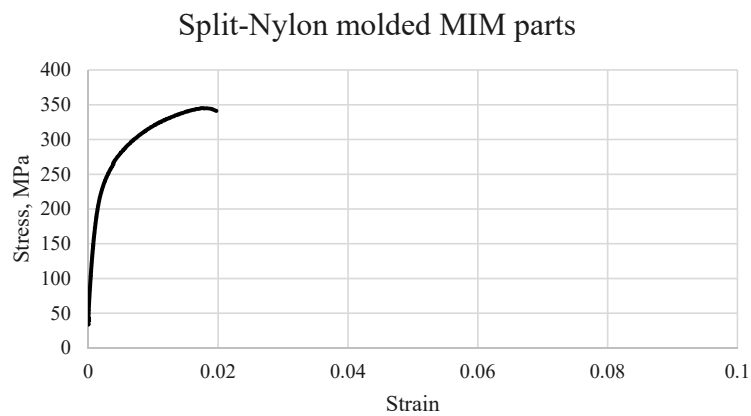
Parameters	Aluminium	Copper-ABS	Split-ABS	Split-Nylon
Peak Stress (MPa)	363.40	284.79	308.93	339.30
Peak Load (kN)	5.73	3.73	5.56	6.10
Yield Strain (%)	0.37	0.33	0.34	0.30
Limit of Proportionality (MPa)	151.49	117.00	151.91	146.93

Figure 12a–d indicates the experimental stress-strain curves for the MIM parts molded with the polymer inserts.

**Figure 12.** *Cont.*



(c)



(d)

Figure 12. Stress-strain graphs of SS 316L molded through (a) aluminum mold insert, (b) copper plated ABS mold insert, (c) ABS Split mold insert, and (d) nylon split mold insert.

Figure 13 indicates the comparison between the molded and sintered parts tensile testing strength with the benchmark part and literature values.

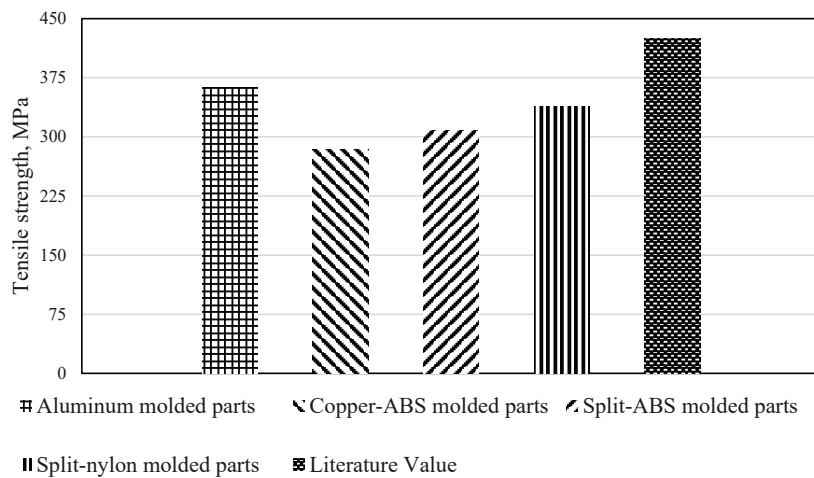


Figure 13. Comparison of tensile strength, and sintered parts with benchmark and literature.

3.3. Hardness Testing

The results obtained from measuring surface hardness of sintered MIM parts are analyzed to investigate the performance of each of mold insert to yield desired surface properties. It was observed that the surface hardness values of MIM parts, made through copper plated ABS and split-nylon mold, were close to parts molded through aluminum mold. However, MIM parts made through split-ABS mold had less hardness number than the others. One possible reason for this could be the uncertainties and fluctuations during the sintering cycle. Figure 14 represents the hardness testing results for sintered parts.

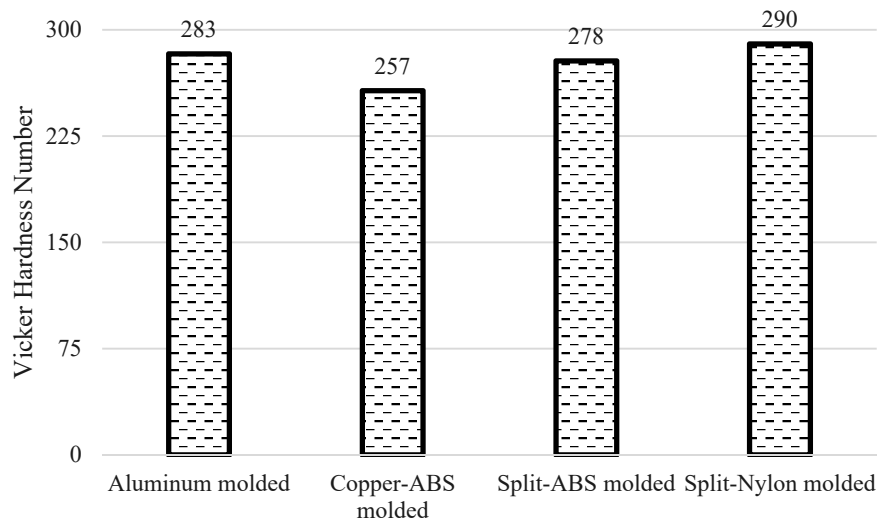


Figure 14. Hardness testing results for sintered parts.

3.4. Density Testing

From the results of density measurement, it can be observed that both the ABS and nylon split mold inserts yield comparable packing and densification of particles compared to benchmark aluminum mold. Sintered density of MIM parts molded using copper-plated ABS mold was slightly less dense. The increase in densification of split mold inserts is attributed to the fact that mold inserts are comparatively elastic and can therefore accommodate sufficient feedstock in themselves, thus contributing to densification. Once mold cavity is filled completely with the feedstock, the mold walls would exert compressive force on the MIM green-part. Hence, these two main factors could have been the factors for better densification of MIM parts. Contrary to split molds, copper-plated ABS mold and metal mold are comparatively rigid, and therefore any filling accompanied by expansion of mold is not prominent. Therefore, densification is less than split mold inserts. Surface of copper-plated ABS mold insert is not as smooth as the split mold inserts of aluminum mold, therefore filling of feedstock is resistive, whereas compaction is only introduced in the molds when filling is complete in all senses. Relatively less compaction and resistive filling are responsible for less density of metal-plated ABS molded sintered parts. However, 87% sintered density is still comparable to other manufacturing and near-net shaping processes. Yet, the sintered density could be improved by troubleshooting and customizing the sintering cycle. The sintering time could be increased further as per the demand of the sintered parts. Figure 15 indicates the density measurement results for the sintered parts compared with benchmark and literature study value.

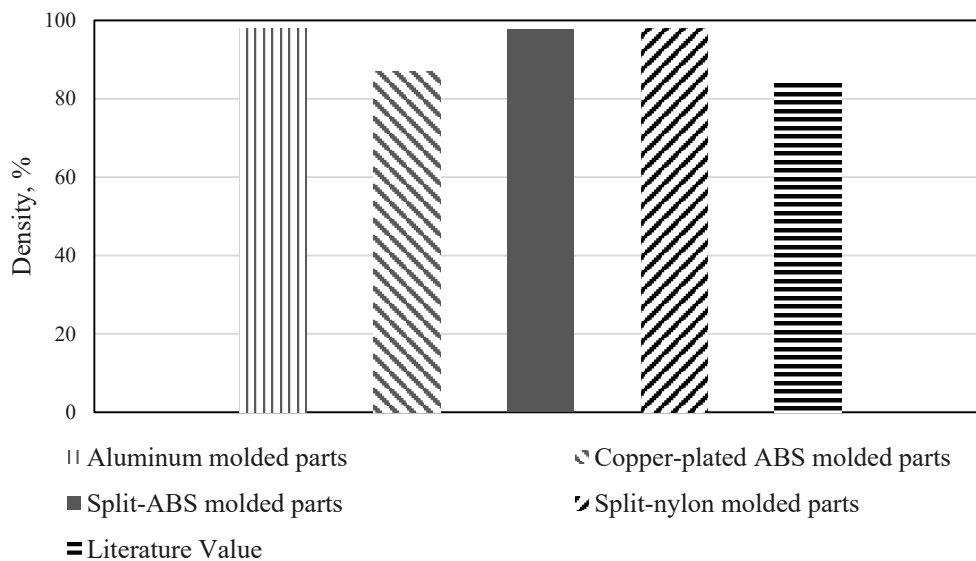


Figure 15. Comparison of densities testing results for sintered parts.

4. Discussion

4.1. Tensile Testing

The MIM parts made through copper-plated ABS mold showed brittle fracture. The part fracture was observed at 284 MPa, compared to the benchmark fracture value of 386 MPa. However, this value is still comparable with some previous powder metallurgy studies, which reported fracture at 290 MPa [24]. Variation in densification could be the reason that the difference appeared in the ultimate strength of copper-plated ABS molded MIM parts, compared to benchmark parts. The densification percentage of 87 in parts molded through copper-plated ABS mold insert was potentially attributed to the relatively rough surface of the plated mold. As the surface roughness increases, the densification is lowered, and thus the mechanical strength decreases.

Parts modeled through split-ABS mold insert possessed ultimate strength of 308 MPa, compared to the benchmark strength of 386 MPa. However, the average yield strength of split-ABS molded MIM parts was calculated to be 147 MPa, compared with the benchmark value of 134 MPa. Despite the fact that ultimate strength of benchmark parts is higher than the split-ABS molded parts, the yield strengths of both cases are comparable. Additionally, the densification percentage of 97.69 is in line with the trend of increased tensile strength.

Split-Nylon molded parts broke at 345 MPa stress, compared to the benchmark strength of 386 MPa. However, it was observed that yield strength of 142 MPa for split-nylon molded parts was slightly higher than the benchmark value of 134 MPa. This implies that split-nylon molded MIM parts were comparable to the benchmark parts. The mechanical strength of MIM parts were observed to be in accordance with their respective densities [25]. The dependence of densification on the tensile strength has also been reported in some other studies. Less densification or porosity influence the mechanical strength in two ways; on one hand they increase the stress concentration in the vicinity of pores, and on the other hand they decrease the effective cross-sectional area. Both of these factors synergistically affect the mechanical properties of the parts. The dependence of mechanical strength on densification has also been reported [26]. Since the manufacturing method inherently alters tensile strength, therefore the unusual difference in mechanical strengths of typical machined SS 316L parts and the specimens under study are attributed to the manufacturing method [15].

4.2. Densification

Too high heating rate is source for thermal shock and could lead to reduction in grain growth, as reported in previous studies [27,28]. Therefore, moderately high heating rate is recommended for proper densification. From literature studies, it is obvious that the sintering density is proportional to the sintering time. The longer the sintering duration, the better would be the density and vice-versa [29].

From literature studies, it is evident that the sintering time and temperature contribute to densification; however, effect of temperature for sintering is more prominent than sintering time. Typical sintered density for SS 316L is of the order of 96–97% [25,30]. This supports the claim that the overall sintering and densification performance is in accordance with the existing relevant studies. However, 87% sintered density in copper-plated ABS molded MIM parts is still comparable to other powder metallurgy processes [25]. Yet, the density could be improved by modifying and customizing the sintering cycle. Figure 16 indicates tensile strength as a function of densities for benchmarked, literature and parts manufactured through FDM polymer molds.

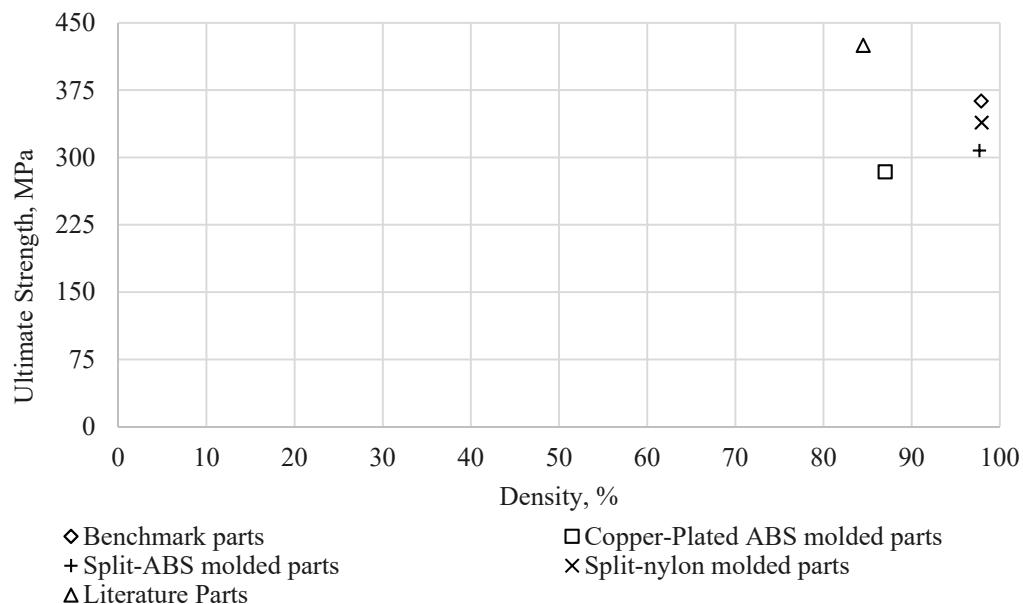


Figure 16. Comparison of tensile strength with density.

5. Conclusions

From the current study, it was observed that FDM printed polymer molds could be used for the MIM process. For a small number of MIM cycles, parts made by ABS and nylon mold inserts were observed to have good performance comparable to the machine metal mold. For low volume part production, prototype manufacturing, design validation, form and fit analysis, and other upstream processes, prior to permanent mold manufacturing, enhanced polymer mold inserts could be a feasible choice in the MIM process.

Author Contributions: Conceptualization and project administration; K.A.; Methodology, writing-review and editing, K.A. and J.A.Q.; Validation; R.M.G. and M.J.; Resources, P.S.M.M.-Y. and F.A.; Investigation and original draft preparation, J.A.Q.; Supervision, K.A., A.M.A.R. and F.A.; Funding acquisition, M.B. and A.R.A.A.

Funding: This research was funded by Universiti Teknologi PETRONAS University Research Internal Fund (URIF), grant number 0153AA-G02.

Acknowledgments: The authors acknowledge technical and financial support from Center of Automotive Research and Electric Mobility (CAREM), Universiti Teknologi PETRONAS (UTP) Malaysia for this study.

Conflicts of Interest: The authors declare no conflict of interest.

References

1. Boparai, K.S.; Singh, R.; Singh, H. Development of rapid tooling using fused deposition modeling: A review. *Rapid Prototyp. J.* **2016**, *22*, 281–299. [[CrossRef](#)]
2. Noble, J.; Walczak, K.; Dornfeld, D. Rapid tooling injection molded prototypes: A case study in artificial photosynthesis technology. *Procedia CIRP* **2014**, *14*, 251–256. [[CrossRef](#)]
3. Dunne, P.; Soe, S.; Byrne, G.; Venus, A.; Wheatley, A. Some demands on rapid prototypes used as master patterns in rapid tooling for injection moulding. *J. Mater. Process. Technol.* **2004**, *150*, 201–207. [[CrossRef](#)]
4. Dixit, U.S.; Joshi, S.N.; Davim, J.P. Incorporation of material behavior in modeling of metal forming and machining processes: A review. *Mater. Des.* **2011**, *32*, 3655–3670. [[CrossRef](#)]
5. Turner, B.N.; Strong, R.; Gold, S.A. A review of melt extrusion additive manufacturing processes: I. Process design and modeling. *Rapid Prototyp. J.* **2014**, *20*, 192–204. [[CrossRef](#)]
6. Kovács, J.G.; Szabó, F.; Kovács, N.K.; Suplicz, A.; Zink, B.; Tábi, T.; Hargitai, H. Thermal simulations and measurements for rapid tool inserts in injection molding applications. *Appl. Therm. Eng.* **2015**, *85*, 44–51. [[CrossRef](#)]
7. Masood, S.; Song, W. Development of new metal/polymer materials for rapid tooling using fused deposition modelling. *Mater. Des.* **2004**, *25*, 587–594. [[CrossRef](#)]
8. Mostafa, N.; Syed, H.M.; Igor, S.; Andrew, G. A study of melt flow analysis of an ABS-Iron composite in fused deposition modelling process. *Tsinghua Sci. Technol.* **2009**, *14*, 29–37. [[CrossRef](#)]
9. Sa'ude, N.; Masood, S.; Nikzad, M.; Ibrahim, M.; Ibrahim, M.H. Dynamic mechanical properties of copper-ABS composites for FDM feedstock. *Int. J. Eng. Res. Appl.* **2013**, *3*, 1257–1263.
10. Novakova-Marcincinova, L.; Kuric, I. Basic and advanced materials for fused deposition modeling rapid prototyping technology. *Manuf. Ind. Eng.* **2012**, *11*, 24–27.
11. Onagoruwa, S.; Bose, S.; Bandyopadhyay, A. Fused deposition of ceramics (FDC) and composites. In Proceedings of the SFF Symposium on Solid Freeform Fabrication, Austin, TX, USA, 6–8 August 2001; pp. 224–231.
12. Ferreira, J.; Mateus, A. Studies of rapid soft tooling with conformal cooling channels for plastic injection moulding. *J. Mater. Process. Technol.* **2003**, *142*, 508–516. [[CrossRef](#)]
13. Altaf, K.; Rani, A.M.A.; Ahmad, F.; Aslam, M. Rapid tooling for powder injection moulding. In Proceedings of the International Conference on Progress in Additive Manufacturing, Singapore, 16–19 May 2016. [[CrossRef](#)]
14. Silva, C.M.A.; Rosa, P.A.R.; Martins, P.A.F. Innovative testing machines and methodologies for the mechanical characterization of materials. *Exp. Tech.* **2014**, *40*, 569–581. [[CrossRef](#)]
15. Krahmer, D.M.; Polvorosa, R.; López de Lacalle, L. Alternatives for Specimen Manufacturing in Tensile Testing of Steel Plates. *Exp. Tech.* **2016**, *40*, 1555–1565. [[CrossRef](#)]
16. Levy, G.N.; Schindel, R.; Kruth, J.P. Rapid Manufacturing and Rapid Tooling with Layer Manufacturing (Lm) Technologies, State Of The Art and Future Perspectives. *CIRP Ann.* **2013**, *52*, 589–609. [[CrossRef](#)]
17. Masood, S.; Song, W.; Hodgkin, J.; Friedl, C. Rapid tooling for injection moulding using fused deposition modelling. In Proceedings of the Society of Plastics Engineers 57th Annual Technical Conference, New York, NY, USA, 2–6 May 1999.
18. King, D.; Tansey, T. Rapid tooling: Selective laser sintering injection tooling. *J. Mater. Process. Technol.* **2003**, *132*, 42–48. [[CrossRef](#)]
19. Afonso, D.; Pires, L.; De Sousa, R.A.; Torcato, R. Direct rapid tooling for polymer processing using sheet metal tools. *Procedia Manuf.* **2017**, *13*, 102–108. [[CrossRef](#)]
20. Qayyum, J.A.; Altaf, K.; Abdul Rani, A.M.; Ahmad, F.; Jahanzaib, M. Performance of 3D printed polymer mold for metal injection molding process. *ARPJ. Eng. Appl. Sci.* **2017**, *12*, 6430–6434.
21. Garcia, A.; Berthelot, T.; Viel, P.; Mesnage, A.; Jégou, P.; Nekelson, F. ABS polymer electroless plating through a one-step poly (acrylic acid) covalent grafting. *ACS Appl. Mater. Interfaces* **2010**, *2*, 1177–1183. [[CrossRef](#)] [[PubMed](#)]
22. Aslam, M. Powder Injection Molding of Modified 316L Stainless Steel for Dental Implant Applications. Ph.D. Thesis, Mechanical Engineering, Universiti Teknologi PETRONAS, Perak, Malaysia, 2016.
23. ASTM. *Standard Test Methods for Tension Testing of Metallic Materials* [Metric]; ASTM E8M-00b; ASTM International: West Conshohocken, PA, USA, 2001; p. 22.

24. Javanbakht, M.; Salahinejad, E.; Hadianfard, M.J. The effect of sintering temperature on the structure and mechanical properties of medical-grade powder metallurgy stainless steels. *Powder Technol.* **2016**, *289*, 37–43. [[CrossRef](#)]
25. Kurgan, N. Effects of sintering atmosphere on microstructure and mechanical property of sintered powder metallurgy 316L stainless steel. *Mater. Des.* **2013**, *52*, 995–998. [[CrossRef](#)]
26. Plessis, A.D.; Yadroitsava, I.; le Roux, S.G.; Yadroitsev, I.; Fieres, J.; Reinhart, C.; Rossouw, P. Prediction of mechanical performance of Ti6Al4V cast alloy based on microCT-based load simulation. *J. Alloys Compd.* **2017**, *724*, 267–274. [[CrossRef](#)]
27. German, R.M. *Sintering Theory and Practice; Solar-Terrestrial Physics (Solnechno-Zemnaya Fizika)*; Wiley: New York, NY, USA; Chichester, UK, 1996; p. 568.
28. Meyers, M.A.; Olevsky, E.A. *Sintering Theory and Practice. J. Mater. Eng. Perform.* **1997**, *6*, 278.
29. German, R.M. *Powder Injection Molding—Design and Applications*; Innovative Material Solutions, Inc.: State College, PA, USA, 2003.
30. Ji, C.; Loh, N.; Khor, K.; Tor, S. Sintering study of 316L stainless steel metal injection molding parts using Taguchi method: Final density. *Mater. Sci. Eng. A* **2001**, *311*, 74–82. [[CrossRef](#)]



© 2018 by the authors. Licensee MDPI, Basel, Switzerland. This article is an open access article distributed under the terms and conditions of the Creative Commons Attribution (CC BY) license (<http://creativecommons.org/licenses/by/4.0/>).